

Selected Spectral Characteristics of Turbulence over an Urbanized Area in the Centre of Łódź, Poland

Krzysztof Fortuniak · Włodzimierz Pawlak

Received: 12 March 2014 / Accepted: 12 August 2014 / Published online: 29 August 2014
© The Author(s) 2014. This article is published with open access at Springerlink.com

Abstract We present the turbulence spectra and cospectra derived from more than five years of eddy-covariance measurements at two urban sites in Łódź, central Poland. The fast response wind velocity components were obtained using sonic anemometers placed on narrow masts at 37 and 42 m above ground level. The analysis follows Kaimal et al. (Q J R Meteorol Soc 98:563–589, 1972) who established the spectral and cospectral properties of turbulent flow in atmospheric surface layer on the basis of the Kansas experiment. Our results illustrate many features similar to those of Kaimal et al., but some differences are also observed. The velocity (co)spectra from Łódź show a clear inertial subrange with $-2/3$ slope for spectra and $-4/3$ slope for cospectra. We found that an appropriate stability function for the non-dimensional dissipation of turbulent kinetic energy calculated from spectra in the inertial subrange differs from that of Kaimal et al., and it can be satisfactorily estimated with the assumption of local equilibrium using standard functions for the non-dimensional shear production. A similar function for the cospectrum corresponds well to Kaimal et al. for unstable and weakly stable conditions. The (co)spectra normalized by their spectral values in the inertial subrange are in general similar to those of Kaimal et al., but they peak at lower frequencies in strongly stable conditions. Moreover, our results do not confirm the existence of a clear “excluded region” at low frequencies for the transition from stable to unstable conditions, for longitudinal and lateral wind components. The empirical models of Kaimal et al. with adjusted parameters fit well to the vertical velocity spectrum and the vertical momentum flux cospectrum. The same type of function should be used for longitudinal and lateral wind spectra because of their sharper peak than occurs for the Kansas data. Finally, it should be stressed that the above relationships are well-defined for averaged values. The results for individual 1-h periods are very scattered and can be significantly different from the generalized functions.

K. Fortuniak (✉) · W. Pawlak
Department of Meteorology and Climatology, Faculty of Geographical Sciences,
University of Łódź, Narutowicza 88, 90-139 Łódź, Poland
e-mail: kfortun@uni.lodz.pl
URL: <http://www.geo.uni.lodz.pl/~meteo/kf~ang.htm>

Keywords Dissipation of turbulent kinetic energy · Eddy-covariance method · Turbulence spectra · Universal functions · Urban climate

1 Introduction

The spectral and cospectral properties of the turbulence over a homogenized flat surface are well established. The most commonly used (co)spectral models in the atmospheric surface layer for such surfaces are those of [Kaimal et al. \(1972\)](#) and [Wyngaard and Coté \(1972\)](#), derived from the Kansas experiment. The universal functions established in this and following experiments are also applied for other types of surface covers, including the urban surface. However, the empirical evidence of their applicability for urban areas is poorly documented. Information on the spectral properties of the flow is essential in many practical problems of air pollution dispersion in urban areas, including the modelling and measurements of turbulent fluxes or other engineering applications. [Roth \(2000\)](#) summarized the studies on urban turbulence in the twentieth century and found that velocity spectra show good agreement with reference spectra. Later, [Feigenwinter et al. \(1999\)](#), [Roth et al. \(2006\)](#), [Vesala et al. \(2008\)](#), [Christen et al. \(2009\)](#) confirmed general agreement between the shape of the spectrum over built-up terrain and a flat, homogeneous surface. Less documented is the dependence of the spectrum on the stability parameter, and the location of the spectrum peak. In particular, there is a lack of empirical verification of the relation of the generalized spectrum on the stability parameter, as was presented in Figs. 3, 4, 5, 6 in [Kaimal et al. \(1972\)](#) and e.g. in [Kaimal and Finnigan \(1994\)](#) and [Sorbján \(1989\)](#). Such an analysis has been done for flows above other types of surfaces, e.g. forest ([Su et al. 2004](#)) or for the South American Pampa ([Moreas 2000](#)).

In the present study, we analyze data from long-term (more than five years) measurements at two urban sites located in Łódź, central Poland, and compare spectral characteristics over the city with the universally accepted functions ([Kaimal et al. 1972](#)). The motivation for such a validation is the differences in the structure of the atmospheric surface layer (ASL) between homogenous flat surfaces and the urban surface. The complex urban geometry makes the lower part of the surface layer, the roughness sub-layer (RSL), thicken over built-up areas, resulting in a relatively thin upper part of the ASL, the inertial sub-layer, where the Monin–Obukhov similarity theory applies. This raises a question about the validity of the universal function in urban areas. Moreover, in the urban ASL, the slope of the spectrum within the inertial subrange can be less than the theoretical $-2/3$ value ([Roth et al. 2006](#)). The reason could be an additional production of eddies in conversion of the mean flow to turbulent energy related to the large range of roughness elements in cities ([Roth et al. 2006](#)). The result will be a smaller spectral roll-off in the inertial subrange. Finally, it should be noted that [Kaimal et al. \(1972\)](#) based their analysis on relatively limited data (15 1-h runs, 10 unstable, 5 stable, at three heights) compared to nearly 86,300 h of measurements from the two sites used in our study.

2 Sites, Data and Processing

Łódź is one of the biggest cities in Poland, located in the centre of the country in relatively flat topography. The built surface of Łódź covers 80km^2 where differences of ground level are no more than 55 m. The present population is about 720,000. The measurement sites are located at the western and eastern edges of the old city centre where buildings were



Fig. 1 Measurement towers at Lipowa (*left*) and Narutowicza (*right*) sites

constructed mainly at the beginning of the twentieth century. The buildings in this region are mostly 15–20 m in height (3–5 storeys) and together with street trees of similar height they form a relatively well-defined roof level. Because of its regular urban structure and a lack of geographical features that could interfere with the urban influences, the city is an excellent location for studies on urban climate. More information on the city's structure and local climate conditions can be found in e.g. [Kłysik \(1996\)](#), [Kłysik and Fortuniak \(1999\)](#), [Fortuniak et al. \(2006, 2013\)](#), and [Zieliński et al. \(2013\)](#).

The first measurement site is located at 81 Lipowa Street ($51^{\circ}45'45''\text{N}$, $19^{\circ}26'43''\text{E}$, 204 m above sea level) in a compact building development with the urban core to the north and the east of the site. The second site is located at 88 Narutowicza Street ($51^{\circ}46'24''\text{N}$, $19^{\circ}28'52''\text{E}$, 221 m above sea level) at a distance of about 2.7 km east from the first one in a slightly less built-up area (Fig. 1). The detailed descriptions of the site surroundings, flux-tower structure, instrumentation, data processing and quality control are given in [Fortuniak et al. \(2013\)](#) for both sites and in [Offerle et al. \(2005, 2006a, b\)](#) and [Pawlak et al. \(2011\)](#) for the Lipowa site only. Hereafter we quote only the key information.

As the urban core lies between the two sites, the building density in the site surroundings is not uniformly distributed. The sectors toward the city centre are more densely built-up. In consequence, the upwind aerodynamic roughness length is also dependent on wind direction with the mean value approximately equal to 2.0 m at Lipowa and 1.9 m at Narutowicza.

The turbulence sensors were installed on top of narrow masts with a top diameter of about 0.1 m. The masts (20 m in height at Lipowa and 25 m at Narutowicza) are mounted on the roof of 3- and 5-storey buildings. The measurement height, z , is equal to 37 m at Lipowa and 42 m at Narutowicza. The average building height, z_H , in the neighbourhood nearest to the measurement sites is 11 m at Lipowa and 16 m at Narutowicza. The related displacement heights, d , calculated from a simple rule of thumb ($d = 0.7 z_H$), can be estimated as 7.7 and 11.2 m, respectively. As the depth of the RSL is typically assessed as 2–4 times the mean building height, it seems to be reasonable to assume that measurements are made in the inertial sub-layer.

At each site, the installed eddy-covariance system consists of an 8100 Young sonic anemometer-thermometer and an open-path gas analyzer (Li7500 infrared $\text{CO}_2/\text{H}_2\text{O}$ gas analyzer at Lipowa and KH20 krypton hygrometer at Narutowicza) connected to a 21X data-

logger (Campbell Scientific, USA) placed on the building below the mast. The data obtained at 10 Hz frequency are computer stored in 15-min files connected via a serial port RS232 to the data logger but, as in [Kaimal et al. \(1972\)](#), hourly records were used here to calculate the (co)spectra and other turbulence characteristics (friction velocity, Obukhov length). Additional data, including the radiation balance components, temperature and humidity or atmospheric pressure are obtained from slow-response sensors.

The data analyzed here were collected from 7 July 2006 to 31 December 2011 at Lipowa (39,807 1-h runs) and from 1 June 2005 to 31 December 2011 at Narutowicza (46,490 1-h runs). For each 1-h run, classical block averaging was used to calculate the fluxes and turbulence statistics. The (co)spectra were calculated on the basis of detrended (linear detrending) data to avoid spurious amplification of lower frequencies (red noise effect). The real part of the cross power spectral density (cpsd) function with the Hamming window (calculated with Matlab cpsd subroutine) was used for (co)spectral estimation in each 1-h period. The original (co)spectra were smoothed by block averaging in 60 bands of the non-dimensional frequency ($f = n(z - d)/U$, where n is natural frequency and U is the local mean wind speed) from 0.001 to 100 of equal width in logarithmic scale. Calculations were made in the natural wind coordinate system with double rotation ([Kaimal and Finnigan 1994](#)). The fluxes, used in Obukhov length estimation, were calculated with the typical procedure for eddy-covariance systems, including covariance maximization in the interval $\pm 2s$, humidity correction for sonic temperature, and the density correction ([Webb et al. 1980](#)).

The pre- and post-processing data quality control was applied to ensure a high quality of the data. The pre-processing procedure included spike detection, threshold values, and the number of good data in each 1-h period. The post-processing data quality control was based on three stationary tests (data were excluded from the analysis even if only one test failed), threshold limits of turbulent fluxes, and rejection of the data for selected wind directions, ϕ , due to distortion of the flow. Data for sectors: $150^\circ < \phi < 320^\circ$ and $030^\circ < \phi < 090^\circ$ for Lipowa and $\phi < 130^\circ$ or $\phi > 340^\circ$ for Narutowicza were excluded. The procedure of data selection was the same as in [Fortuniak et al. \(2013\)](#) and details about stationary tests and discussion on rejection of the data for selected wind directions can be found there.

3 Spectral and Cospectral Characteristics

The three classical regions can be distinguished in the turbulent part of the atmospheric energy spectrum ([Kaimal and Finnigan 1994](#)): the energy-containing range, where energy is produced by buoyancy and shear, the inertial subrange, and the dissipation range. According to the Kolmogorov theory for the inertial subrange, the one-dimensional spectrum, $S_i(n)$, of any wind component, $i = (u, v, w)$, normalized by the squared friction velocity, u_*^2 , may be expressed in the form

$$\frac{nS_i(n)}{u_*^2} = \frac{\alpha_i}{(2\pi\kappa)^{2/3}} \phi_\varepsilon^{2/3}(\zeta) f^{-2/3} = a_i \phi_\varepsilon^{2/3}(\zeta) f^{-2/3}, \quad (1)$$

where n is the natural frequency, f is the non-dimensional frequency, $\alpha_i = (\alpha_u, \alpha_v, \alpha_w)$ are universal Kolmogorov inertial subrange constants and $a_i = \alpha_i/(2\pi\kappa)^{2/3}$, with κ being the von Kármán constant, $\phi_\varepsilon(\zeta)$ is a non-dimensional dissipation rate of turbulent kinetic energy (TKE), ε . The ϕ_ε is a function of stability parameter, $\zeta = (z - d)/L$, where L is the Obukhov length.

Both α_i and ϕ_ε must be determined empirically from spectral measurements. The Kolmogorov constant for longitudinal wind component, α_u , ranges from 0.36 to 0.56 ([Högström](#)

1990). As a consequence of isotropy, α_v and α_w should be both equal to $4/3 \alpha_u$. Kaimal et al. (1972) estimate the constants $a_i = \alpha_i / (2\pi\kappa)^{2/3}$ as $a_u = 0.3$ and $a_v = a_w = 0.4$ with 10% accuracy and no clear dependency on ζ .

The non-dimensional dissipation rate of TKE, ϕ_ε , is related to other universal functions via the normalized TKE budget (Kaimal and Finnigan 1994),

$$\phi_m - z/L - \phi_t - \phi_p - \phi_\varepsilon = 0, \tag{2}$$

where ϕ_m is shear production, $-z/L$ is buoyant production, ϕ_t is turbulent transport, and ϕ_p is pressure transport. The common assumption that the sum of turbulence and pressure transport is negligible (local equilibrium), leads to the simplification

$$\phi_\varepsilon = \phi_m - z/L, \tag{3}$$

which suggests the general form of the ϕ_ε related to the better known ϕ_m . However, there is some empirical evidence that production is not locally dissipated (Högström 1990; Frenzen and Vogel 1992, 2001; Albertson et al. 1997; Pahlow et al. 2001; Li et al. 2008) and Eq. 3 should be modified to

$$\phi_\varepsilon = \psi(\phi_m - z/L), \tag{4}$$

where $\psi = \phi_\varepsilon(\zeta = 0)$ is referred to as the imbalance coefficient varying in the range from 0.61 to 1.24 (Li et al. 2008). Still, the functional form of the non-dimensional dissipation rate of TKE can be derived on the basis of the dimensionless wind shear function, ϕ_m .

Högström (1990) applied the assumption that $\phi_\varepsilon = \phi_m - \zeta$ with $\phi_m = (1 - 19 \zeta)^{-1/4}$ to obtain a form of ϕ_ε . For a convective case ($\zeta < 0$), he found $\phi_\varepsilon = 1.24[(1 - 19\zeta)^{-1/4} - \zeta]$, while Su et al. (2004) proposed a more general function based on the assumption of local equilibrium,

$$\phi_\varepsilon^{2/3}(\zeta) = [(1 - c_1\zeta)^{p_1} - c_2\zeta]^{2/3}, \quad \zeta < 0, \tag{5}$$

where c_1 and c_2 are empirically fitted parameters, and $p_1 = -1/4$. They found that c_1 ranges from 25.5 to 129.0 and c_2 from 0.59 to 1.43. The assumption of local equilibrium (Eq. 3) was recently confirmed by Charuchittipan and Wilson (2009) with the dimensionless wind-shear function based on Dyer and Bradley (1982), $\phi_m = (1 - 28\zeta)^{-1/4}$. In addition, they concluded that the absence of local equilibrium could be a result of uncertainty in the Kolmogorov coefficient. The general form of ϕ_ε given by Eq. 5 is also used in sensible heat-flux estimations with the scintillometer. For rural areas Thiermann and Grassl (1992) suggest $c_1 = 3$, $c_2 = 1$, and $p_1 = -1$, whereas for urban areas Kanda et al. (2002) estimate these parameters as $c_1 = 10.5$, $c_2 = 1$, and $p_1 = -1$, and Roth et al. (2006) use $\phi_\varepsilon = (0.93 - 5.4\zeta)^{-1.1} - 2\zeta$, for measurements above rooftops. All these functions differ from that proposed by Wyngaard et al. (1971) on the basis of Kansas data,

$$\phi_\varepsilon^{2/3}(\zeta) = 1 + c_3(-\zeta)^{2/3}, \quad \zeta < 0, \tag{6}$$

with parameter c_3 initially found to be 0.5, and later reported to be 0.75 (Caughey and Wyngaard 1979). The same function was used by McBean and Elliot (1975) and Champagne et al. (1977). Garratt (1972) suggested for ϕ_ε the same form as for the non-dimensional shear production ϕ_m . Other methods of functional description of the experimental data of ϕ_ε include a translated and rotated hyperbola (Frenzen and Vogel 2001) or a three sub-layer model for the convective case (Albertson et al. 1997).

For stable stratification, ϕ_m usually takes the form of a linear function of the stability parameter (Kaimal and Finnigan 1994; Sorbjan 1989). Thus, assuming that local equilibrium and a_i do not change with stability, one can expect ϕ_ε to be a linear function of ζ ,

$$\phi_\varepsilon^{2/3}(\zeta) = (1 + b_1\zeta)^{2/3}, \quad \zeta > 0. \tag{7}$$

The empirically fitted parameter, b_1 is estimated as $b_1 = 3.7$ (Garratt 1972), $b_1 = 4.0$ (Wyngaard 1975), $b_1 = 5.0$ (Kaimal and Finnigan 1994) and $b_1 = 3.79$ (Högström 1990). Again this form differs from the ‘classical’ one,

$$\phi_\varepsilon^{2/3}(\zeta) = 1 + b_2\zeta^{3/5}, \quad \zeta > 0, \tag{8}$$

with $b_2 = 2.5$ given by Wyngaard et al. (1971).

Similar to the velocity spectra, the inertial subrange cospectrum, $Co_{uw}(n)$, of the vertical momentum flux has the form

$$-\frac{nCo_{uw}(n)}{u_*^2} = \frac{\alpha_{uw}}{(2\pi\kappa)^{4/3}} \phi_m(\zeta)\phi_\varepsilon^{1/3}(\zeta)f^{-4/3} = a_{uw}G_{uw}(\zeta)f^{-4/3}. \tag{9}$$

Wyngaard and Coté (1972) predicted that α_{uw} approaches a constant value in the free convection limits. Using the observed empirical functions of ϕ_m and ϕ_ε , they found that the right-hand side of Eq. 9 becomes $a_{uw}f^{-4/3}$ for unstable conditions with $a_{uw} = 0.043$. Kaimal et al. (1972) used a slightly higher value $a_{uw} = 0.048$. In stable conditions, they estimated G_{uw} to be proportional to ζ ,

$$G_{uw}(\zeta) = 1 + b_{uw}\zeta, \quad 0 < \zeta < 2, \tag{10}$$

with $b_{uw} = 7.9$. Su et al. (2004) reported a_{uw} from the range 0.024–0.055, and also found that Eq. 10 holds only when $\zeta < 0.5$. For $\zeta > 0.5$, the stability function increases less rapidly with ζ , so they propose the relation

$$G_{uw}(\zeta) = 1 + c_{uw}\zeta^{p_{uw}}, \quad 0 < \zeta < 2, \tag{11}$$

with parameter c_{uw} varying between 4.13 and 13.02 and p_{uw} between 0.49 and 0.72.

The similarity expressed by Eq. 1 allows for the normalization of u , v , and w spectra by ϕ_ε , which removes their dependence on ζ and brings all spectra into coincidence in the inertial subrange. The generalized spectral curves obtained this way by Kaimal et al. (1972) show some important characteristics: (1) For $\zeta > 0$, the spectral intensity peak is reduced and shifted to higher frequencies as stability increases; (2) no particular dependence of spectral peak on static stability is observed for $\zeta < 0$ in the case of u and v spectra and for $\zeta < -0.3$ for the w spectrum; (3) a curious “excluded region” separates the stable and unstable spectra in the case of u and v velocity components; (4) the unstable v spectrum has two distinguishable regimes: the first for $f \geq 0.2$, where it follows the shape of the neutral spectrum, and the second for $f < 0.2$, dominated by a large peak in the range $0.005 < f < 0.2$. Similar two regions, but not so clearly distinguishable, can be found in the unstable u spectrum.

The unique behaviour of the u and v spectra in the energy-containing region for $\zeta < 0$ suggests that some length scale other than z controls the low-frequency spectral behaviour in the horizontal velocity components. A simple model incorporates the depth of the convective boundary layer, z_i , as an additional scaling variable (Kaimal 1978; Højstrup 1981; McNaughton et al. 2007; Choi et al. 2011). According to Højstrup (1981), the horizontal velocity spectra, $S(n)$, can be written as a sum of the low-frequency part, $S_L(n)$, which is entirely buoyancy produced, and the high-frequency part, $S_M(n)$, which is shear produced. It is assumed that there is little interaction between the two parts, sufficient for modelling them

separately. The low-frequency part is a function of non-dimensional frequency, $f_i = nz_i/L$; the high-frequency part is the neutral limit from the stable side. The final forms of for the u and v velocity component spectra can be expressed as

$$\frac{nS_u(n)}{u_*^2} = \frac{0.5 f_i}{1 + 2.2 f_i^{5/3}} \left(\frac{z_i}{-L} \right)^{2/3} + \frac{105 f}{(1 + 33 f)^{5/3}}, \tag{12a}$$

$$\frac{nS_v(n)}{u_*^2} = \frac{0.32 f_i}{1 + 1.1 f_i^{5/3}} \left(\frac{z_i}{-L} \right)^{2/3} + \frac{17 f}{(1 + 9.5 f)^{5/3}}, \tag{12b}$$

where the first and the second part of the right-hand sides are the low- and high-frequency components, respectively. The model well describes the shape of the empirical horizontal spectra. However, in contradiction to the Kansas results, no “excluded region” in transition from the neutral limit approached from the stable side to the unstable spectrum is predicted. Instead, a rapid variation in the spectral shape from neutral towards slightly unstable conditions is predicted by the model. Højstrup (1981) also proposed a two-part model of the w spectrum in unstable conditions. Both parts are scaled with ζ ,

$$\frac{nS_w(n)}{u_*^2} = \frac{32 f}{(1 + 17 f)^{5/3}} (-\zeta)^{2/3} + \frac{2 f}{1 + 5.3 f^{5/3}}, \tag{12c}$$

and the second part is again a spectrum in the neutral limit from the stable side. Such an approach explains both that the spectrum peak shifts to the lower frequencies as instability increases and that it becomes less sharp in such conditions.

Similarly to the spectral functions, the normalization of the cospectrum Co_{uw} by $a_{uw}G_{uw}$ brings all cospectral functions to a single curve in the inertial region. In stable situations, the normalized cospectral functions exhibit a shift of the peak to higher frequencies as stability increases. The normalized unstable cospectra converge to a relatively narrow band. The universal curves based on Kaimal et al. (1972) for near-neutral situations takes the form (Kaimal and Finnigan 1994)

$$- \frac{nCo_{uw}(n)}{u_*^2} = \frac{12 f}{(1 + 9.6 f)^{7/3}}. \tag{13}$$

The frequency of the spectrum peak maximum, f_m , and the related wavelength $\lambda_m = z/f_m$ show a regular dependence on stability for $\zeta > 0$ for all velocity components, while only the w component shows some dependence also for $\zeta < 0$. Kaimal et al. (1972) estimated that $f_{m,w} \approx 5 f_{m,u} \approx 2 f_{m,v}$ for $\zeta > 0$. In the unstable case, the frequency of the w spectrum peak initially decreases for increased instability and next stabilizes at a constant value of about 0.17 when $\zeta < -1$. Kaimal and Finnigan (1994) propose a linear approximations of $f_{m,w}$ according to stability regimes,

$$f_{m,w} = \left\{ \begin{array}{ll} 0.55 + 0.38\zeta, & 0 > \zeta > -1 \\ 0.17, & \zeta < -1 \end{array} \right\} \tag{14a}$$

$$f_{m,w} = \left\{ \begin{array}{ll} 0.55 + \zeta, & 0 \leq \zeta \leq 1 \\ 1.1 + 0.45\zeta, & 1 \leq \zeta \leq 2 \\ \zeta, & \zeta \geq 2 \end{array} \right\} \tag{14b}$$

4 Results and Discussion

4.1 The Spectra of Velocity Components

The empirical spectra of wind components in Łódź show strong similarities in shape with Eq. 1 in the high frequency region. Basing on the spectral analysis only, we were not able to evaluate separately the values of a_i and $\phi_\varepsilon(\zeta)$. Instead, we estimated the products of the non-dimensional dissipation rates of TKE and universal constants, $a_i\phi_\varepsilon(\zeta)$. They were calculated by a least-squares fit of the power function, $y = Ax^b$, to the measured inertial subrange of the velocity spectra. We used the data for the frequency range $4 < f < 10$, while Kaimal et al. (1972) calculated them at $f = 4$. Other authors used two (e.g. $f = 4$ and 5, Su et al. 2004) or more (e.g. $4 < f < 10$, Zhang and Park 1999) frequencies to obtain $a_u\phi_\varepsilon^{2/3}(\zeta)$, $a_v\phi_\varepsilon^{2/3}(\zeta)$ and $a_w\phi_\varepsilon^{2/3}(\zeta)$. The parameter b in the relation $y = Ax^b$ was used as an additional data quality criterion in the ϕ_ε estimation. The data chosen for the analysis fulfilled the condition $-0.72 < b < -0.63$ (the spectral slope deviated less than 8% from the theoretical $-2/3$ slope).

To evaluate $a_u\phi_\varepsilon^{2/3}(0)$, $a_v\phi_\varepsilon^{2/3}(0)$ and $a_w\phi_\varepsilon^{2/3}(0)$ the empirical data were smoothed by moving averages and the crossing of this line with $\zeta = 0$ determined values at neutral stability. The values of the products are similar at both sites. The values of a_v/a_u ($a_v/a_u = 1.33$ and $a_v/a_u = 1.35$ for Lipowa and Narutowicza respectively) are close to the $4/3$ value as predicted by isotropy. Our results for a_w/a_u ($a_w/a_u = 1.11$ and $a_w/a_u = 1.13$) are lower than predicted by isotropy, but they are consistent with other works. Values of a_w/a_u lower than $4/3$ were observed in many studies, especially for rough surfaces such as forest (Anderson et al. 1986; Amiro 1990; Su et al. 2004) or (sub)urban areas, where the values of a_w/a_u range from 1.03 to 1.20 as reported by Roth and Oke (1993), Roth et al. (2006), and Christen et al. (2009). Höglström et al. (1982) found in Uppsala the a_w/a_u ratio close to $4/3$ for measurements at a height of 50 m, and 1.15 and 1.06 for sensors mounted at lower heights. Feigenwinter et al. (1999) report a_w/a_u around 1.2 for measurements at different levels above the urban canopy in Basel.

Taking the assumption that $\phi_\varepsilon(0) = 1$, the values of the products $a_i\phi_\varepsilon^{2/3}(0)$ determine a_i . The constants a_i estimated in this way for Łódź are close to those given by Kaimal et al. (1972) for the longitudinal and transverse wind components and lower for the vertical wind component: $a_i\phi_\varepsilon^{2/3}(0) = 0.320, 0.425$, and 0.355 for the u, v, w components at Lipowa and $0.310, 0.420, 0.350$ at Narutowicza. The uncertainties in the von Kármán constant and the universal Kolmogorov inertial subrange constants make the validation of the assumption $\phi_\varepsilon(0) = 1$ impossible. The extensive observations since the 1960s have shown that the values of κ range from 0.32 to 0.43. Some studies (e.g. Oncley et al. 1996; Frenzen and Vogel 2001; Andreas et al. 2006; Li et al. 2008; Leonardi and Castro 2010; Kanda et al. 2013) suggest that κ could be lower than 0.4, especially over rough surfaces (κ decreases with increasing roughness Reynolds number). The Kolmogorov constant, α_u , also ranges from 0.36 to 0.56 (Höglström 1990), which introduces additional imprecision in the estimation of $\phi_\varepsilon(0)$. For example, when taking $\alpha_u = 0.54$ and $\kappa = 0.365$ after Oncley et al. (1996), our data give $\phi_\varepsilon(0) = 1$ in the limits of the estimation error. Whereas taking $\alpha_u = 0.52$ and $\kappa = 0.4$ after Höglström (1990) and following his argumentation, we estimate $\phi_\varepsilon(0) = 1.21$ for the Lipowa site and $\phi_\varepsilon(0) = 1.16$ for Narutowicza, which could be interpreted as the local dissipation is 21% and 16% respectively larger than the local production.

To evaluate $\phi_\varepsilon^{2/3}(\zeta)$ as an empirical function of ζ , we divided $a_i\phi_\varepsilon^{2/3}(\zeta)$ by its neutral value $a_i\phi_\varepsilon^{2/3}(0)$ so that the empirical functions are equal to 1 at $\zeta = 1$ (Fig. 2). The original

data are scattered, but their stability dependence is clear. A preliminary analysis, carried out separately on the wind components (u , v , w) and two sites, showed no clear, regular differences between the wind components, so we decided to analyze all the data together to obtain more statistically reliable results.

For unstable conditions, the normalized ϕ_ε first decreases to a minimum approximately at $\zeta = -0.2$ and next increases with a more negative ζ . The same general shape of the ϕ_ε function has been reported previously (e.g. Högström 1990; Zhang and Park 1999; Frenzen and Vogel 2001; Su et al. 2004; McNaughton 2006; Roth et al. 2006). For urbanized areas, the dip observed between $\zeta = -0.5$ and -0.1 is more pronounced in the data from Tokyo and Vancouver analyzed by Kanda et al. (2002) than in our studies, whereas data from Basel (Roth et al. 2006) show only a slight decrease for measurements above the roof level ($z/z_H = 1.32$). The last square fit of the function defined by Eq. 5 to our data with fixed parameter $p_1 = -1/4$ gives

$$\phi_\varepsilon^{2/3}(\zeta) = [(1 - 37\zeta)^{-1/4} - \zeta]^{2/3}, \quad \zeta < 0. \quad (15)$$

We chose to use a fixed value of the parameter p_1 as the exponent $-1/4$ is most commonly used in the definition of the function ϕ_m . The value of parameter $c_1 = 37$ is greater than the corresponding values used most frequently for the ϕ_m function. However, a visual comparison of our fit with other estimations directly employing ϕ_m shows that the plots are virtually indistinguishable (Fig. 2b). Moreover, the use of other forms of ϕ_m also fit well the data from Łódź. This result and the value of the parameter $c_2 = 1$ confirm the close relationship of ϕ_ε and ϕ_m function defined by Eq. 3 (or more generally by Eq. 4) and its applicability for an urbanized area (at least in the case of Łódź). Surprisingly, the functions developed especially for urban areas generally do not match our data so well as other functions. The function proposed by Kanda et al. (2002) systematically underestimates our values by about 0.3, while the function suggested by Roth et al. (2006) increases much more rapidly than our data as ζ becomes more negative.

In the stable case, the ϕ_ε estimated from the Łódź data almost linearly increases with stability, thus a linear model (Eq. 7) is fitted to the data. Our approximation of $b_1 = 3.45$ is lower than the value deduced from $\phi_\varepsilon = \phi_m - \zeta$ for a typical range of slopes of ϕ_m in stable stratification (e.g. Table 1 in Li et al. 2008). The majority of other studies report higher values for this parameter. However, Hartogensis and De Bruin (2005) found even lower values of b_1 based on the CASES-99 experiment. They pointed out several possible reasons for lower values of ϕ_ε in stable and very stable conditions, including: inaccuracies in the von Kármán and Kolmogorov constants, a short averaging period (they used 5-min time intervals to exclude non-turbulent contributions), and a limited number of data for very stable conditions in previous studies. They also found no equilibrium between the dissipation and production rates of TKE ($\phi_\varepsilon(0) \neq 1$). Su et al. (2004) also recorded lower values of the parameter b_1 in several cases of measurements over a forest. The function of the type given by Eq. 8, in our case $\phi_\varepsilon^{2/3}(\zeta)/\phi_\varepsilon^{2/3}(0) = 1 + 1.56\zeta^{3/5}$, fits slightly better to the data for $0 < \zeta < 0.5$ but fails in more stable conditions. The use of functions with a greater number of free parameters provides an even better fit to the measurements, e.g. in our case the function $\phi_\varepsilon^{2/3}(\zeta)/\phi_\varepsilon^{2/3}(0) = 1 + 1.64\zeta^{0.72}$ works reasonably well, but the large spread of measurement points puts into question the advisability of such a procedure (the degree of fitting is higher, but generalization is lost). The high data scatter could be related to the self-correlation effect that cannot be avoided when using MOST scaling (e.g. Hicks 1978; De Bruin et al. 1993). Klipp and Mahrt (2004) and Baas et al. (2006) showed that ϕ_m is influenced by this effect; both the high scatter and the increase, less rapid than linear, of ϕ_m with stability in very

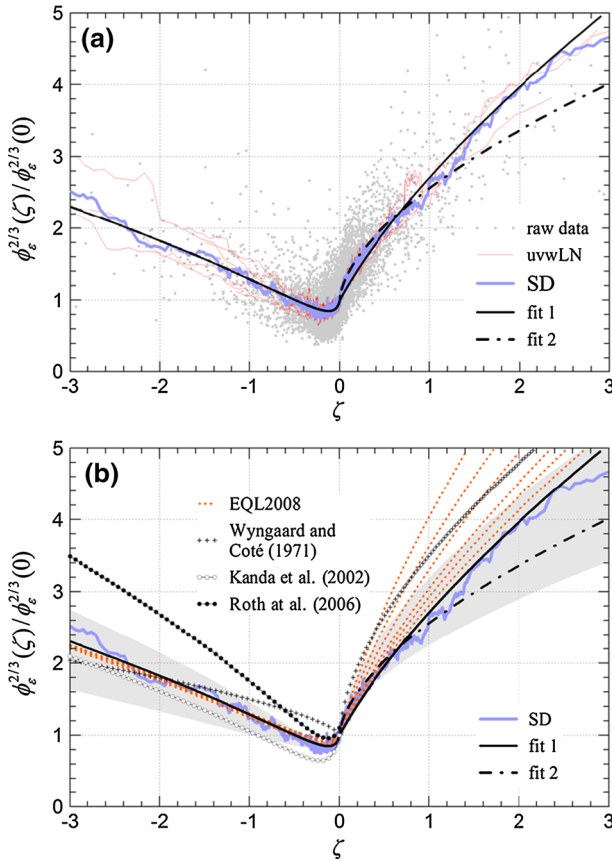


Fig. 2 Estimated stability function $\phi_\epsilon^{2/3}(\zeta)/\phi_\epsilon^{2/3}(0)$ plotted against the stability parameter $\zeta = (z - d)/L$. *Upper panel a* dots original data for 1-h period for all wind components (u, v, w) for two sites in Łódź; uvwLN—band-averaged function calculated separately for each wind component and for each site; SD—band-averaged function from all data; fit 1—the function $\phi_\epsilon = (1 - 37\zeta)^{-1/4} - \zeta$ (for $\zeta < 0$), $\phi_\epsilon = 1 + 3.45\zeta$ (for $\zeta > 0$); fit 2—the function $\phi_\epsilon^{2/3} = 1 + 1.56\zeta^{3/5}$ (for $\zeta > 0$); *Low panel b* EQL2008—different form of ϕ_ϵ calculated as $\phi_\epsilon = \phi_m - \zeta$ with various ϕ_m taken after Table 1 by Li et al. (2008); grey area—range of results Su et al. 2004

stable conditions can be a spurious result of self-correlation between variables due to the occurrence of the friction velocity on both axes. In our case, the friction velocity also affects both variables. Even if its relation with ϕ_ϵ is not as straightforward as in the case of ϕ_m , the non-linearity of ϕ_ϵ for large ζ could be forced by self-correlation. However, Hartogensis and De Bruin (2005) proved that spurious correlation does not determine the shape of the ϕ_ϵ function, but only affects the scatter of the data. The same was shown for ϕ_m by Baas et al. (2006). A detailed exploration of the self-correlation effect in the ϕ_ϵ estimation is beyond the scope of this study; however, our experiments with randomizing the input data ($\phi_\epsilon, u_*, w/T'$) and with renormalization of the variables similar to that presented by Klipp and Mahrt (2004) and Baas et al. (2006) do not lead to a consistent conclusion on the influence of self-correlation on the shape of the ϕ_ϵ function. Depending on the method of testing, the role of spurious correlation seems to be less or more important, but in general it must be considered as a source of uncertainty.

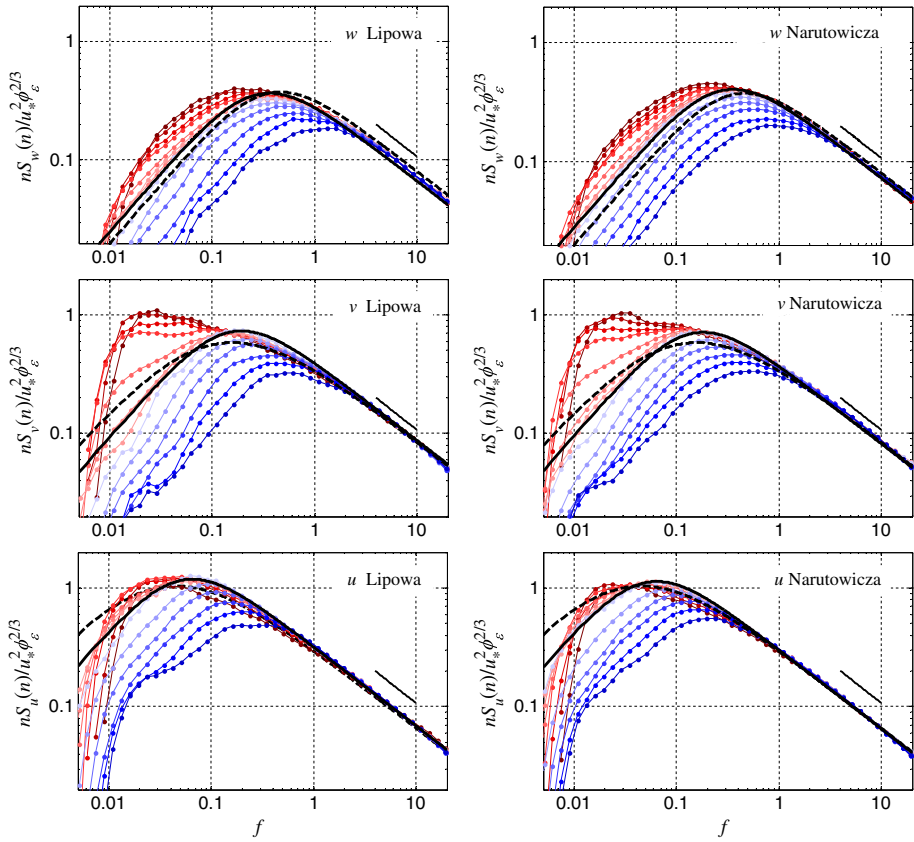


Fig. 3 Normalized logarithmic w, v, u spectra plotted against the non-dimensional frequency, $f = n(z-d)/U$ for Lipowa (left) and Narutowicza (right) sites for stability classes listed in Table 1. Red colours indicate unstable cases (more dark red—more unstable), blue colours indicate stable cases (more dark blue—more stable). Short dark solid lines indicate the $-2/3$ slope and range over which spectra were normalized. Thin solid black line—fitted model for statically neutral stratification (Eqs. 18); dashed black line—model based on the Kansas data (second term in right side of Eqs. 12)

The velocity spectra from Łódź, normalized by $\phi_\epsilon^{2/3}$ and u_*^2 , are presented in Fig. 3. We evaluated the spectra for 13 stability categories as a median over the number of cases listed in Table 1; the large number of data allowed for detailed studies of the separation of the spectra in close to neutral regimes. Our neutral limits from the stable side include the spectra from the narrow stability band $0 < \zeta < 0.01$ (similarly, in the unstable limit) as compared to the relatively wide band ($0 < \zeta < 0.1$) used by Kaimal et al. (1972).

The normalized spectra from Łódź illustrate many characteristics similar to those of Kaimal et al. (1972). They converge to a single line in the inertial subrange and have their maximum at a lower frequency; in the inertial subrange, they follow the $-2/3$ slope quite well. The separation according to ζ is clear in statically stable conditions for all velocity components: the increased stability results in a reduction of the spectral intensity peak and its shift to higher frequencies. The same general rule of spectrum evolution is also pronounced in statically unstable conditions for the vertical velocity component. Similar to the Kansas data, the unstable v velocity spectrum has two regimes separated by the normalized frequency of

Table 1 Number of cases, N , used in calculation of the median spectrum and median value of stability parameter, ζ , for each stability range presented in Fig. 3

Stability range	N Lipowa	Median ζ Lipowa	N Narutowicza	Median ζ Narutowicza
$-1.4 < \zeta < -0.6$	117	-0.80	301	-0.81
$-0.65 < \zeta < -0.35$	222	-0.45	443	-0.47
$-0.35 < \zeta < -0.25$	220	-0.29	379	-0.29
$-0.25 < \zeta < -0.15$	457	-0.19	673	-0.19
$-0.15 < \zeta < -0.05$	897	-0.09	1406	-0.09
$-0.05 < \zeta < -0.01$	634	-0.03	1106	-0.03
$-0.01 < \zeta < 0$	89	-0.007	195	-0.006
$0 < \zeta < 0.01$	44	0.007	154	0.006
$0.01 < \zeta < 0.05$	206	0.03	815	0.03
$0.05 < \zeta < 0.15$	263	0.08	1004	0.10
$0.15 < \zeta < 0.35$	187	0.22	568	0.22
$0.35 < \zeta < 0.65$	61	0.45	294	0.46
$0.6 < \zeta < 1.4$	42	0.78	266	0.84

the spectral peak in the neutral limit, which is in our case about 0.18 for Lipowa and 0.16 for Narutowicza. Its value, lower than in the Kansas data, is probably a result of averaging over closer to neutral stability—our spectra for the stability category $0.01 < \zeta < 0.05$ peak at $f \approx 0.2$. The separation between the v spectra approaching the neutral limit from the stable and unstable sides at lower frequencies is very narrow in our case. As we use closer to neutral categories for spectrum averaging, it suggests a continuous transition from the stable to unstable regime rather than the existence of an “excluded region”. No clear “excluded region” has been recently reported for different natural surfaces (Moreas 2000; Su et al. 2004; Choi et al. 2011), either. The evolution of the v spectrum shape with ζ at low frequencies for $\zeta < 0$ is qualitatively well predicted by the Højstrup (1981) model. As we have not measured the height of the boundary layer, we are not able to evaluate this model using our data. However, the increased contribution of the (low-frequency) buoyancy produced part of the spectrum reaching the maximum at frequencies in the range 0.01–0.03 is clear for v spectra for $\zeta < -0.2$. It should be pointed out that the 1-h period used for individual spectral calculations may act as a high-pass filter that artificially amplifies the spectral roll-off at low frequencies.

All the unstable u spectra at both sites in Łódź collapse into a relatively narrow band; for a weakly unstable case, the frequency of the spectrum peak shifts slightly to lower frequencies as instability increases. The results concerning the excluded region are not as consistent as in the v case. Similar to the v spectrum, the excluded region is hardly detected for the u spectrum at the Narutowicza site, but it appears at the Lipowa site. However, a more detailed inspection for narrowed ζ bands ($-0.005 < \zeta < 0$ and $0 < \zeta < 0.005$) shows a smooth transition from stable to unstable conditions.

The analytical expressions of the spectrum in the neutral limit from the stable side given by the second part of the right-hand side of Eq. 12 are commonly used for a comparison of different experimental and laboratory data, as well as for different engineering applications. They fit quite well the data from Łódź (dashed black lines in Fig. 3) in the w and v cases. Still, the spectrum of the transverse flow exhibits a sharper peak than given by Eq. 12b. For the

longitudinal flow, the curve given by Eq. 12a fits the unstable spectra rather than the neutral limits. Testing two analytical functions used to describe spectra in the entire frequency range,

$$\frac{nS_i(n)}{u_*^2} = \frac{\beta_1 f}{1 + \beta_2 f^{5/3}}, \tag{16}$$

and

$$\frac{nS_i(n)}{u_*^2} = \frac{\beta_3 f}{(1 + \beta_4 f)^{5/3}}, \tag{17}$$

we found the first form more appropriate not only for the w spectrum but also for the v and u spectra. The empirical models of the spectrum for the neutral limit ($0 < \zeta < 0.005$) with the parameters fitted by the least-squares method take the forms

$$\frac{nS_u(n)}{u_*^2} = \frac{45 f}{1 + 140 f^{5/3}}, \text{ and } \frac{nS_u(n)}{u_*^2} = \frac{44 f}{1 + 145 f^{5/3}}, \tag{18a}$$

$$\frac{nS_v(n)}{u_*^2} = \frac{9.4 f}{1 + 23 f^{5/3}}, \text{ and } \frac{nS_v(n)}{u_*^2} = \frac{9.7 f}{1 + 25 f^{5/3}}, \tag{18b}$$

$$\frac{nS_w(n)}{u_*^2} = \frac{2.5 f}{1 + 8.0 f^{5/3}}, \text{ and } \frac{nS_w(n)}{u_*^2} = \frac{2.8 f}{1 + 8.2 f^{5/3}}, \tag{18c}$$

for Lipowa and Narutowicza, respectively.

The dependence of the location of the spectral peak, f_m , on stability, ζ (Fig. 4) was tested by finding the maximum of the function $y = ax/(1+bx^{5/3})$ fitted to the spectrum for each 1-h period. The original data are quite scattered, so the median and the 25th and 75th percentiles were calculated for the selected ζ bands. The median values show a clear dependence on the stability parameter both for the vertical and horizontal velocity components. In general, they follow the curves of Kaimal et al. (1972). The approximation $f_{m,w} \approx 5 f_{m,u} \approx 2 f_{m,v}$ is roughly met in the stable domain, while a more precise estimation gives: $f_{m,w} \approx 5.0 f_{m,u} \approx 1.8 f_{m,v}$ both for the Lipowa and Narutowicza sites. The values of f_m for close-to-neutral stratification for the w, v, u components are respectively equal to: 0.35, 0.17, and 0.065 at the Lipowa site and 0.32, 0.15, and 0.052 (estimation based on the extrapolation of mean values to $\zeta = 0$) at the Narutowicza site, which are slightly lower than estimated on the basis of the Kansas experiment. The increase of f_m for $\zeta > 0$ is at first more rapid and then slower than in the reference data. This suggests that, in contrast to Eq. 14, the relation of f_m to ζ , for $\zeta > 0$ is not linear but takes the form of $f_m \sim \zeta^C$ with $0 < C < 1$. We use a function of the type

$$f_m = A_1 + A_2 \zeta^C, \tag{19}$$

with parameters A_1, A_2 , and C fitted to the median values by the least-squares method (Table 2). A slower shift of the spectrum peak to higher frequencies for strong stability can be a consequence of the rough urban geometry. The surface of a city is characterized by large objects of the size of several to tens of metres (buildings, structures, etc.) which even in strongly stable stratification make the dominating eddies large compared to those over a flat surface.

In unstable conditions, the reasonable estimation of the dependence of f_m on ζ can be done for the vertical component only. Our results indicate that median values for the horizontal wind components also show some kind of relationship, but the data are randomly spread in a wide band, which prevents a reasonable estimation of the characteristic size of dominating eddies. Moreover, the double maximum of the v and u spectra makes the estimation of the location of each individual spectral peak uncertain. The $f_{m,w}$ for the data from Łódź reach

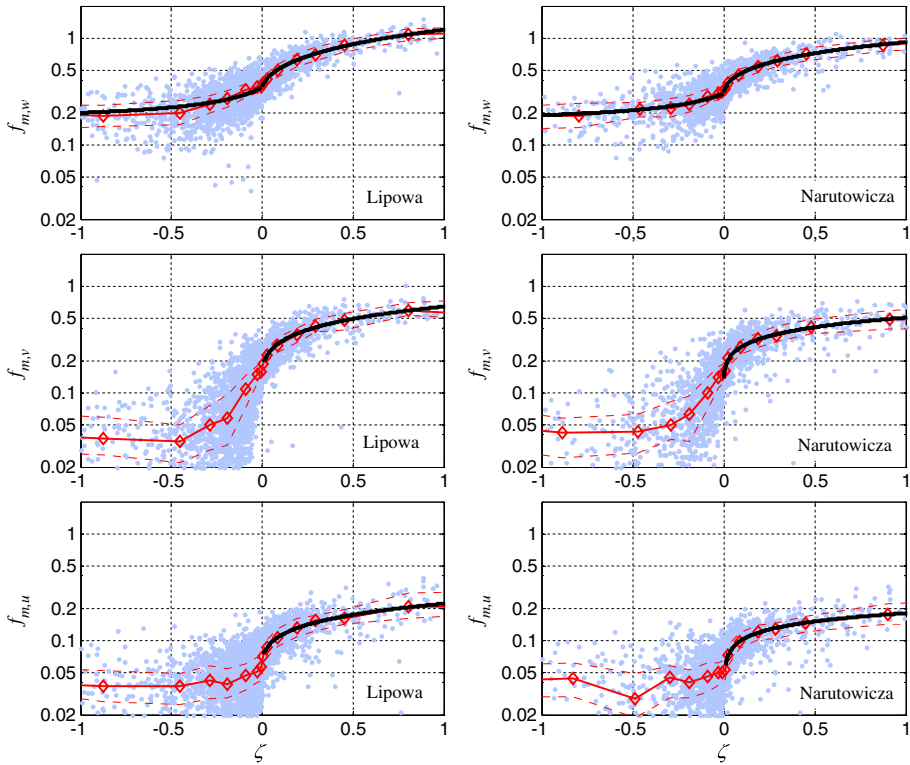


Fig. 4 Logarithmic spectral peak for w, v and u wind component plotted against the stability parameter $\zeta = (z - d)/L$ for the Lipowa and Narutowicza sites. *Blue dots* represent original data for 1-h periods; *red solid line*—median value of f_m in stability bands; *dashed red line*—25th and 75th percentiles; *thick black line*—fitted functions (Eqs. 19 and 20)

Table 2 Empirical coefficients of the function $f_m = A_1 + A_2 \zeta^C$ fitted to the median values of spectral and cospectral peak location, f_m , on the stability, ζ , at the Lipowa and Narutowicza sites

	Lipowa			Narutowicza		
	A_1	A_2	C	A_1	A_2	C
$f_{m,w}$	0.34	0.85	0.68	0.29	0.62	0.55
$f_{m,v}$	0.15	0.49	0.52	0.11	0.39	0.40
$f_{m,u}$	0.058	0.16	0.49	0.012	0.17	0.029
$f_{m,uw}$	0.086	0.46	0.75	0.082	0.31	0.64

the free convection limits faster than in the reference rural case; the median values of $f_{m,w}$ stabilize at the level of $f_{m,w} \approx 0.18$ for $\zeta < -0.5$. The limit values can be estimated by a hyperbolic fit to the data and we use the function

$$f_{m,w} = -1/(B_1 + B_2\zeta) + B_3, \tag{20}$$

with parameters B_1 and B_2 fitted with the least-squares method. Parameter B_3 , which implies the limit of $f_{m,w}$ for $\zeta \rightarrow -\infty$, is determined by the value of the function for $\zeta = 0$ and parameter B_1 : $B_3 = f_{m,w}(0) + 1/B_1$. The estimated values of the parameters B are close:

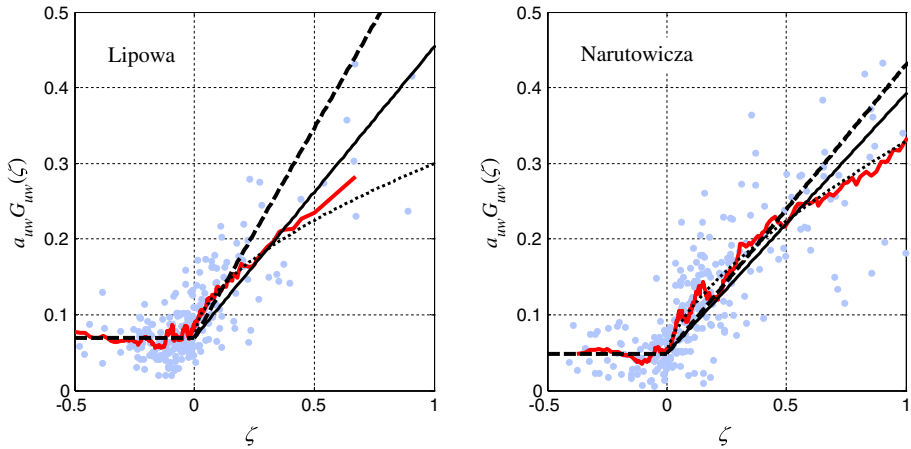


Fig. 5 Estimated $a_{uw}G_{uw}(\zeta)$ using measured cospectra for $2 < f < 6$ at two sites in Łódź. Blue points represent original data for 1-h periods; red solid line—band averaged data; black dashed line—Kaimal et al. (1972) model of G_{uw} ; black solid line—linear fit (Eq. 10); black dotted line—power fit (Eq. 11)

$B_1 = 21$ and 22 , $B_2 = -5.5$ and -6.8 , $B_3 = 0.16$ and 0.15 for Lipowa and Narutowicza, respectively.

4.2 The Cospectra of Vertical Momentum Flux

The empirical cospectra, $-nCo_{uw}(n)/u_*^2$ are not as well formed as the empirical spectral functions. Occasional negative values might influence the spectral shape, and so the requirement of positive values of $-nCo_{uw}(n)/u_*^2$ for $0.1 < f < 10$ is used as an additional restriction for the data selection in the cospectral analysis. Moreover, the estimation of the product $a_{uw}G_{uw}$ is based only on the data with the cospectral slope in the inertial subrange on a log-log plot varying between -1.5 and -1.2 , which is close to the $-4/3$ value predicted by similarity theory. As in the estimation of ϕ_ε , the product $a_{uw}G_{uw}$ was found by fitting the power function to the cospectrum in the inertial subrange, here defined as $2 < f < 6$, because of the faster decline of Co_{uw} than in the case of spectral functions.

The calculated $a_{uw}G_{uw}$ values for the selected cases of 1-h periods are presented in Fig. 5. The individual data are, again, very scattered and the data selection significantly reduces the total number of analyzed cases. Still, the averaged curves confirm the general dependence of $a_{uw}G_{uw}$ on stability. At both sites, $a_{uw}G_{uw}$ is constant for $\zeta < 0$, and its mean is the same as given by Kaimal et al. (1972) at Narutowicza ($a_{uw} = 0.048$) and higher at Lipowa ($a_{uw} = 0.070$). In stable conditions, the linear approximation given by Eq. 10 is applicable only for small ζ ; the function proposed by Kaimal et al. (1972) can be used for $\zeta < 0.5$ at Narutowicza and $\zeta < 0.2$ at Lipowa. A linear fit to the Łódź data for $0 < \zeta < 1$ gives smaller values of parameter b_{uw} ($b_{uw} = 5.5$ at Lipowa and $b_{uw} = 7.1$ at Narutowicza). The power functions: $G_{uw} = 1 + 3.3\zeta^{0.57}$ for Lipowa and $G_{uw} = 1 + 5.8\zeta^{0.68}$ for Narutowicza (Eq. 11), fit the averaged data better, but the final conclusion about the type of functional dependence of G_{uw} on ζ must be drawn with caution. The agreement with the Kaimal et al. (1972) model is good as long as the average functions are estimated on the basis of a reasonably large number of data points. Discrepancies appear only for estimations based on a few strongly scattered points.

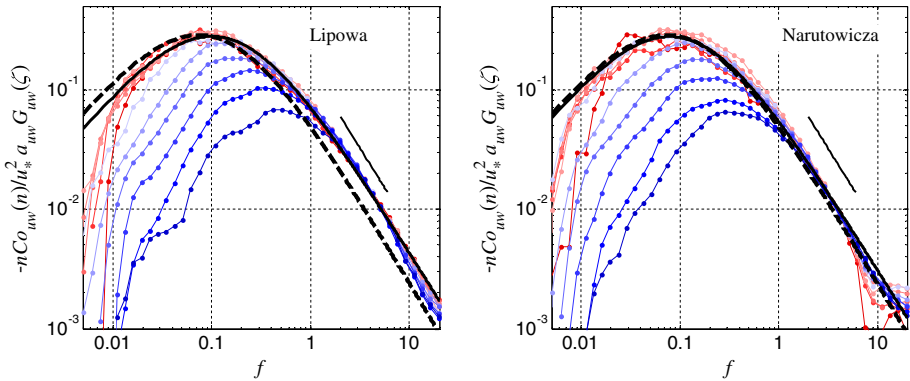


Fig. 6 Normalized logarithmic uw cospectrum plotted against f for Lipowa (left) and Narutowicza (right) sites for stability classes listed in Table 1. Red colours indicate unstable cases (more dark red—more unstable), blue colours indicate stable cases (more dark blue—more stable). Short dark solid lines indicate the $-4/3$ slope and range over which spectra were normalized. Thin solid black line—fitted model for statically neutral stratification (Eq. 21); dashed black line—Kaimal and Finnigan (1994) model

The stress cospectra normalized by $a_{uw}G_{uw}$ (Fig. 6) demonstrate many characteristics typical of those presented by Kaimal et al. (1972); they converge to a single line in the inertial subrange and follow the $-4/3$ law; the separation according to ζ is evident in the statically stable state; the cospectral peak is reduced and shifted to higher frequencies as stability increases. The cospectra for the statically unstable state fall in a relatively narrow band determined by the neutral limit from the unstable side. As in the us spectrum case, the cospectra in the neutral limit from the stable and unstable sides are indistinguishable at Narutowicza but converge at low frequencies at Lipowa.

The analytical relation (Eq. 13) given by Kaimal and Finnigan (1994) fits well the statically neutral and unstable cospectra at the Narutowicza site but underestimates the spectra in the inertial sub-region at the Lipowa site. The least-squares fit of the function of the type given by Eq. 13 to the empirical cospectra (for frequencies $0.01 < f < 10$) gives

$$\frac{nC_{uw}(n)}{u_*^2} = \frac{10.2f}{(1 + 7.4f)^{7/3}}, \tag{21a}$$

and

$$\frac{nC_{uw}(n)}{u_*^2} = \frac{12.9f}{(1 + 9.5f)^{7/3}}, \tag{21b}$$

for Lipowa and Narutowicza, respectively.

Similarly to the analysis of the spectrum peak, the dependence of the location of the cospectral peak, $f_{m,uv}$, on stability, ζ , (Fig. 7) was tested by finding the maximum of the function $y = ax/(1 + bx)^{7/3}$ fitted to the cospectrum for each 1-h period. Again, the large scatter of the individual results requires averaging of the data. The median values in the statically stable case confirm a general increase of $f_{m,uv}$ with stability, but less rapid than in the Kansas data. The fit of the power function given by Eq. 19 to the $f_{m,uv}$ data for $0 < \zeta < 1$ gives an exponent < 1 both for the Lipowa and Narutowicza data (Table 2). In the statically unstable case, the median location of the cospectrum peak remains at a constant level, slightly higher than 0.08, but the data are highly scattered in the band $0.02 < f_{m,uv} < 0.2$.

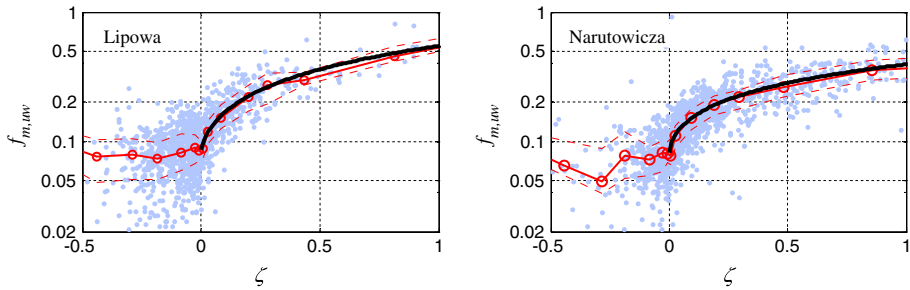


Fig. 7 The same as Fig. 4 but for the uw cospectral peak

5 Summary and Conclusions

The turbulent spectra and cospectra of wind-velocity components above the top of an urban roughness sub-layer have been analyzed at two urban sites (Lipowa and Narutowicza) in Łódź, central Poland. The results are based on eddy-covariance data collected between July 2006 and December 2011 at Lipowa and between June 2005 and December 2011 at Narutowicza analyzed in 1-h periods.

The normalized spectra and cospectra from Łódź show many similar characteristics to the classical results for a homogenous flat surface reported by Kaimal et al. (1972) for the Kansas experiment. Nevertheless, even after a careful data quality verification, these relationships become clear only in averaged (co)spectra and universal functions. The results for individual 1-h periods are very scattered and can be significantly different from the generalized dependences.

The inertial subrange is clear both in the spectra and cospectra from Łódź with a $-2/3$ slope for spectra and a $-4/3$ slope for cospectra. The ratio of the lateral to longitudinal velocity spectral densities in the inertial subrange is very close to the $4/3$ value predicted by isotropy, but as in many other studies for rough surfaces, the ratio of the vertical to longitudinal spectral densities is smaller.

The product of the universal constant and the non-dimensional dissipation rate of TKE, ϕ_ε , was calculated from the spectra in the inertial subrange. The results from Łódź show that ϕ_ε divided by its neutral value can be estimated from the normalized TKE budget with the assumption of local equilibrium, $\phi_\varepsilon = \phi_m - \zeta$, using standard functions for the non-dimensional shear production, ϕ_m . In the unstable case, our data fit very well the function evaluated in this way, much better than for other estimations of ϕ_ε based on data from urbanized areas. In the stable case, the different forms of ϕ_m reported in the literature make the comparisons more problematic. In general, the data from Łódź show a slower increase of ϕ_ε with stability for $\zeta > 0$. Still, it seems that there is no reason to reject a general conclusion on the applicability of the relation $\phi_\varepsilon = \phi_m - \zeta$. A similar universal function, G_{uw} , for the cospectrum of the vertical momentum flux follows the Kansas data for the statically unstable and weakly stable case (it remains constant for $\zeta < 0$ and increases linearly for a small positive ζ). The increase is less rapid for a stronger stability, but the fact that the median is calculated on the basis of a small number of data points does not allow for a definitive conclusion about the type of relationship in this stability region.

The velocity (co)spectra from Łódź normalized by their value in the inertial sub-range illustrate most of the characteristics found by Kaimal et al. (1972). The shift of the (co)spectral peak to higher frequencies as stability increases is clear in the statically stable case, but

for strong stability the increase of the frequency of (co)spectral maximum, f_m , with ζ is slower than for a flat surface. It can be attributed to the specific urban surfaces, where various obstacles contribute to relatively large vortex generation even in statically stable stratification. The spectra from Łódź for the u and v wind components do not show a clear “excluded region” at low frequencies in the transition from stable to unstable stratification qualitatively described by the Højstrup (1981) model. As Kaimal et al. (1972) used wider bands of ζ in averaging spectra for close to neutral stratification, it is possible that the “excluded region” is a simple consequence of this procedure.

The analytical models of the neutral spectrum in the entire frequency range given by Kaimal et al. (1972) fits quite well the data from Łódź in the case of the vertical wind component, but the fitted constants differ from the reference values. The same type of functional dependence should be used for the spectra of the longitudinal and lateral velocity components. The function proposed by Kaimal et al. (1972) for horizontal flows is in general too flat. The empirical cospectra of the vertical momentum flux from Łódź fit the Kaimal et al. (1972) model, but at the Lipowa site the empirical values in the inertial subrange are slightly higher.

The general conclusion from our findings is that, in spite of some differences, the spectral and cospectral properties of the flow at the top of the urban roughness sub-layer are very similar to those for homogenous flat terrain and many universal functions found for such surfaces can be directly applied over urbanized areas.

In spite of differences in constants, we found that the analytical model of the neutral spectrum in the entire frequency range given by Kaimal et al. (1972) fits quite well the urban data in the case of the vertical wind component.

Acknowledgments Funding for this research was provided by the Polish Ministry of Science and Higher Education (State Committee for Scientific Research) under grant no. N306 276935 for the years 2008–2012 and grant no. N306 519638 for the years 2010–2013.

Open Access This article is distributed under the terms of the Creative Commons Attribution License which permits any use, distribution, and reproduction in any medium, provided the original author(s) and the source are credited.

References

- Albertson JD, Parlange MB, Kiely G, Eichinger WE (1997) The average dissipation rate of turbulent kinetic energy in the neutral and unstable atmospheric surface layer. *J Geophys Res* 102:13423–13432
- Amiro BD (1990) Drag coefficients and turbulence spectra within three boreal forest canopies. *Boundary-Layer Meteorol* 52:227–246
- Anderson DE, Verma SB, Clement RJ (1986) Turbulent spectra of CO₂, water vapour, temperature and velocity over a deciduous forest. *Agric For Meteorol* 38:81–99
- Andreas EL, Claffey KJ, Jordan RE, Fairall CW, Guest PS, Persson CW, Grachev AA (2006) Evaluations of the von Kármán constant in the atmospheric surface layer. *J Fluid Mech* 559:117–149
- Baas P, Steeneveld GJ, van de Wiel BJH, Holtslag AAM (2006) Exploring self-correlation in flux-gradient relationships for stably stratified conditions. *J Atmos Sci* 63:3045–3054
- Caughey SJ, Wyngaard JC (1979) The turbulent kinetic energy budget in convective conditions. *Q J R Meteorol Soc* 105:231–239
- Champagne FH, Friche CA, LaRue JC, Wyngaard JC (1977) Flux measurements, flux estimation techniques, and fine-scale measurements in the unstable surface layer over land. *J Atmos Sci* 34:515–530
- Charuchittipan D, Wilson JD (2009) Turbulent kinetic energy dissipation in the surface layer. *Boundary-Layer Meteorol* 132:193–204
- Choi W, Faloona IC, McKay M, Goldstein AH, Baker B (2011) Estimating the atmospheric boundary layer height over sloped, forested terrain from surface spectral analysis during BEARPEX. *Atmos Chem Phys* 11:6837–6853

- Christen A, Rotach MW, Vogt R (2009) The budget of turbulent kinetic energy in the urban roughness sublayer. *Boundary-Layer Meteorol* 131:193–222
- De Bruin HAR, Kohsiek W, Van den Hurk BJJM (1993) A verification of some methods to determine the fluxes of momentum, sensible heat and water vapour using standard deviation and structure parameter of scalar meteorological quantities. *Boundary-Layer Meteorol* 63:231–257
- Dyer A, Bradley E (1982) An alternative analysis of flux-gradient relationships at the 1976 ITCE. *Boundary-Layer Meteorol* 22:3–19
- Feigenwinter C, Vogt R, Parlow E (1999) Vertical structure of selected turbulence characteristics above an urban canopy. *Theor Appl Climatol* 62:51–63
- Fortuniak K, Klysik K, Wibig J (2006) Urban-rural contrasts of meteorological parameters in Łódź. *Theor Appl Climatol* 84:91–101
- Fortuniak K, Pawlak W, Siedlecki M (2013) Integral turbulence statistics over a central European city centre. *Boundary-Layer Meteorol* 146:257–276
- Frenzen P, Vogel CA (1992) The turbulent kinetic energy budget in the atmospheric surface layer: a review and an experimental reexamination in the field. *Boundary-Layer Meteorol* 60:49–76
- Frenzen P, Vogel CA (2001) Further studies of atmospheric turbulence in layers near the surface: scaling the TKE budget above the roughness sublayer. *Boundary-Layer Meteorol* 99:173–206
- Garratt JR (1972) Studies of turbulence in the surface layer over water. *Q J R Meteorol Soc* 98:642–657
- Hartogensis OK, De Bruin HAR (2005) Monin–Obukhov similarity functions of the structure parameter of temperature and turbulent kinetic energy dissipation rate in the stable boundary layer. *Boundary-Layer Meteorol* 116:253–276
- Hicks BB (1978) Some limitations of dimensional analysis and power laws. *Boundary-Layer Meteorol* 14:567–569
- Högström U (1990) Analysis of turbulence structures in the surface layer with a modified similarity formulation for near neutral conditions. *J Atmos Sci* 47:1949–1972
- Högström U, Bergström H, Alexandersson H (1982) Turbulence characteristics in a near neutrally stratified urban atmosphere. *Boundary-Layer Meteorol* 23:449–472
- Højstrup J (1981) A simple model for the adjustment of velocity spectra in unstable conditions downstream of an abrupt change in roughness and heat flux. *Boundary-Layer Meteorol* 21:341–356
- Kaimal JC (1978) Horizontal velocity spectra in an unstable surface-layer. *J Atmos Sci* 35:18–24
- Kaimal JC, Finnigan JJ (1994) Atmospheric boundary layer flows: their structure and measurement. Oxford University Press, New York 289 pp
- Kaimal JC, Wyngaard JC, Coté OR (1972) Spectral characteristics of surface-layer turbulence. *Q J R Meteorol Soc* 98:563–589
- Kanda M, Moriwaki R, Roth M, Oke TR (2002) Area-averaged sensible heat flux and a new method to determine zero-plane displacement length over an urban surface using scintillometry. *Boundary-Layer Meteorol* 105:177–193
- Kanda M, Inagaki A, Miyamoto T, Gryschka M, Raasch S (2013) A new aerodynamic parametrization for real urban surfaces. *Boundary-Layer Meteorol* 143:357–377
- Klipp CL, Mahrt L (2004) Flux-gradient relationship, self-correlation and intermittency in the stable boundary layer. *Q J R Meteorol Soc* 130:2087–2103
- Klysik K (1996) Spatial and seasonal distribution of anthropogenic heat emissions in Lodz, Poland. *Atmos Environ* 30:3397–3404
- Klysik K, Fortuniak K (1999) Temporal and spatial characteristics of the urban heat island of Łódź, Poland. *Atmos Environ* 33:3885–3895
- Leonardi S, Castro IP (2010) Channel flow over large cube roughness: a direct numerical simulation study. *J Fluid Mech* 651:519–539
- Li X, Zimmerman N, Princevac M (2008) Local imbalance of turbulent kinetic energy in the surface layer. *Boundary-Layer Meteorol* 129:115–136
- McBean GA, Elliot JA (1975) Vertical transports of kinetic energy by turbulence and pressure in the boundary layer. *J Atmos Sci* 32:753–766
- McNaughton KG (2006) On the kinetic energy budget of the unstable atmospheric surface layer. *Boundary-Layer Meteorol* 118:83–107
- McNaughton KG, Clement RJ, Moncrieff JB (2007) Scaling properties of velocity and temperature spectra above the surface friction layer in a convective atmospheric boundary layer. *Nonlinear Process Geophys* 14:257–271
- Moreas OLL (2000) Turbulence characteristics in the surface boundary layer over the South American Pampa. *Boundary-Layer Meteorol* 96:317–335
- Offerle B, Grimmond CSB, Fortuniak K (2005) Heat storage and anthropogenic heat flux in relation to the energy balance of a central European city centre. *Int J Climatol* 25:1405–1419

- Offerle B, Grimmond CSB, Fortuniak K, Kfysik K, Oke TR (2006a) Temporal variations in heat fluxes over a central European city centre. *Theor Appl Climatol* 84:103–115
- Offerle B, Grimmond CSB, Fortuniak K, Pawlak W (2006b) Intra-urban differences of surface energy fluxes in a central European city. *J Appl Meteorol Climatol* 45:125–136
- Oncley SP, Friehe CA, Larue JC, Businger JA, Itsweire EC, Chang SS (1996) Surface-layer fluxes, profiles, and turbulence measurements over uniform terrain under near-neutral conditions. *J Atmos Sci* 53:1029–1044
- Pahlow M, Parlange M, Porté-Agel F (2001) On Monin–Obukhov similarity in the stable atmospheric boundary layer. *Boundary-Layer Meteorol* 99:225–248
- Pawlak W, Fortuniak K, Siedlecki M (2011) Carbon dioxide flux in the centre of Łódź, Poland—analysis of a 2-year eddy covariance measurement data set. *Int J Climatol* 31:232–243
- Roth M (2000) Review of atmospheric turbulence over cities. *Q J R Meteorol Soc* 126:941–990
- Roth M, Oke TR (1993) Turbulent transfer relationships over an urban surface. I: spectral characteristics. *Q J R Meteorol Soc* 119:1071–1104
- Roth M, Salmond JA, Satyanarayana ANV (2006) Methodological considerations regarding the measurement of turbulent fluxes in the urban roughness sublayer: the role of scintillometry. *Boundary-Layer Meteorol* 121:351–375
- Sorbjan Z (1989) *Structure of the atmospheric boundary layer*. Prentice Hall, Englewood Cliffs, NJ 317 pp
- Su HB, Schmid HP, Grimmond CSB, Vogel CS, Oliphant AJ (2004) Spectral characteristics and correction of long-term eddy-covariance measurements over two mixed hardwood forests in non-flat terrain. *Boundary-Layer Meteorol* 110:213–253
- Thiermann V, Grassl H (1992) The measurement of turbulent surface-layer fluxes by use of bichromatic scintillation. *Boundary-Layer Meteorol* 58:367–389
- Vesala T, Järvi L, Launiainen S, Sogachev A, Rannik Ü, Mammarella I, Siivola E, Keronen P, Rinne J, Riikonen A, Nikinmaa E (2008) Surface-atmosphere interactions over complex urban terrain in Helsinki, Finland. *Tellus B* 60:188–199
- Webb EK, Pearman GI, Leuning R (1980) Correction of flux measurements for density effects due to heat and water vapor transfer. *Q J R Meteorol Soc* 106:85–100
- Wyngaard JC (1975) Modeling the planetary boundary—extension to the stable case. *Boundary-Layer Meteorol* 9:441–460
- Wyngaard JC, Coté OR (1972) Cospectral similarity in the atmospheric surface layer. *Q J R Meteorol Soc* 98:590–603
- Wyngaard JC, Coté OR, Izumi Y (1971) Local free convection, similarity, and the budgets of shear stress and heat flux. *J Atmos Sci* 28:1171–1182
- Zhang H-S, Park S-U (1999) Dissipation rates of turbulent kinetic energy and temperature and humidity variances over different surfaces. *Atmos Res* 50:37–51
- Zieliński M, Fortuniak K, Pawlak W, Siedlecki M (2013) Turbulent sensible heat flux in Łódź, Central Poland, obtained from scintillometer and eddy covariance measurements. *Meteorol Z* 22:603–613